Chaos, Solitons and Fractals 165 (2022) 112820

Contents lists available at ScienceDirect

Chaos, Solitons and Fractals

journal homepage: www.elsevier.com/locate/chaos

From absolute equilibrium to Kardar–Parisi–Zhang crossover: A short review of recent developments

Marc Brachet *

Laboratoire de Physique de l'Ecole Normale Supérieure, ENS, Université PSL, France
CNRS, Sorbonne Université, Université de Paris, F-75005 Paris, France

ARTICLE INFO

Keywords:
Interface growth
Kardar–Parisi–Zhang
Crossover
Spectrally truncated hydrodynamics
Burgers equation
Superfluidity

ABSTRACT

I first recall the theoretical background relevant to spectral truncation: absolute equilibrium in helical flows and compressible effects. Thermalization phenomenology in Gross–Pitaevskii superflows and thermalization processes in classical systems are then briefly reviewed. The so-called 'tygers' that appear in the truncated inviscid Burgers equation are demonstrated. The basic definitions that relate the Burgers equation to the Kardar–Parisi–Zhang system are recalled. Spectral truncation and conserved quantities are used to introduce the microcanonical and canonical stationary probabilities. The main results on the crossover from absolute equilibrium to Kardar–Parisi–Zhang scaling are finally given after a brief discussion of the relevant physical parameters. The present contribution is thus a short review of the publications, scientific developments and collaborations that went on during the last decade and led to the joint work (Cartes et al., 2022) that I presented at the XVIII Instabilities and Nonequilibrium Structures Workshop held (online) in December 2021 in Valparaiso (Chile), dedicated to the memory of the late Enrique Tirapegui.

1. Introduction

Time-reversible spectrally-truncated hydrodynamical systems, retaining only a finite number of Fourier modes, have been studied actively in fluid mechanics [1–5]. T. D. Lee, in his 1952 pioneering work [1], showed that these truncated systems satisfy Liouville's theorem and that (assuming ergodicity) there is energy equipartition among the spectral modes. A different approach was proposed later by Kraichnan [4] for these *absolute equilibrium* states by considering that the complex amplitudes of the Fourier modes followed a canonical distribution, controlled by the mean values of the invariants of the system.

The present short review is dedicated to the memory of Enrique Tirapegui. It takes as a starting point the situation described in our previous paper on absolute equilibrium of Galerkin truncated flows that was published in 2009 [6]. In this reference, we introduced a new algorithm to construct absolute equilibrium of spectrally truncated *compressible* flows. This new algorithm allowed us to generalize to the compressible case results that were previously known only for incompressible flows. During the decade that followed, scientific collaborations went on and finally led to the joint work that was published in Ref. [7] and presented at the XVIII Instabilities and Nonequilibrium Structures Workshop held (online) in December 2021 in Valparaiso (Chile). A common point shared by the works reviewed here is that they involve absolute equilibrium in the presence of compressible effects (or, more generally, waves).

The paper is organized as follows. In Section 2, after an introduction to the theoretical background needed to understand spectral truncation and absolute equilibrium of helical flows, the algorithm introduced in Ref. [6] is recalled. The various topics to which these methods were applied are then reviewed: thermalization in the Gross–Pitaevskii equation, applications of thermalization process to classical systems and, finally, the so-called 'tygers' that appear in the thermalization of the truncated inviscid Burgers equation. Section 3 is devoted to the collaboration that led to the publication of Ref. [7]. After recalling the basic definitions that relate the Burgers equation to the Kardar–Parisi–Zhang system, the spectral truncation and conserved quantities are reviewed to introduce the corresponding stationary probability. After a brief discussion of the physical parameters the main results on the crossover are given. Finally Section 4 is the conclusion.

* Correspondence to: Laboratoire de Physique de l'Ecole Normale Supérieure, ENS, Université PSL, France.
E-mail address: marc-etienne.brachet@phys.ens.fr.

https://doi.org/10.1016/j.chaos.2022.112820
Received 22 June 2022; Received in revised form 13 October 2022; Accepted 16 October 2022
Available online 3 November 2022

2. From incompressible flows to the Burgers equation

2.1. Spectral truncation and absolute equilibrium

The spectrally-truncated hydrodynamical system that was most extensively studied is the $3D$ Euler equation

$$\partial_t \mathbf{u} + (\mathbf{u}\cdot\nabla)\,\mathbf{u} = -\nabla p$$
$$\nabla\cdot\mathbf{u} = 0, \tag{1}$$

for a classical, ideal fluid which can be studied efficiently, in a spatially periodic domain, by the Fourier pseudospectral method [8,9].

With spherical spectral truncation performed at wave-number $k_{\rm max}$ (1) yields [10,11] the following finite system of ordinary differential equations for the Fourier transform of the velocity $\hat{\mathbf{u}}(\mathbf{k})$ ($\mathbf{k}$ is a $3D$ vector of relative integers satisfying $|\mathbf{k}| \le k_{\rm max}$):

$$\partial_t \hat{u}_\alpha(\mathbf{k},t) = -\frac{i}{2}\mathcal{P}_{\alpha\beta\gamma}(\mathbf{k})\sum_{\mathbf{p}} \hat{u}_\beta(\mathbf{p},t)\hat{u}_\gamma(\mathbf{k}-\mathbf{p},t), \tag{2}$$

where $\mathcal{P}_{\alpha\beta\gamma} = k_\beta P_{\alpha\gamma} + k_\gamma P_{\alpha\beta}$ with $P_{\alpha\beta} = \delta_{\alpha\beta} - k_\alpha k_\beta/k^2$ and repeated indices are summed over.

This finite number of ordinary differential equations is a time-reversible system that exactly conserves both energy $E = \sum_k E(k,t)$ and helicity $H = \sum_k H(k,t)$, where energy $E(k,t)$ and helicity $H(k,t)$ spectra are defined by integrating respectively $\frac{1}{2}|\hat{\mathbf{u}}(\mathbf{k}',t)|^2$ and $\hat{\mathbf{u}}(\mathbf{k}',t)\cdot\hat{\boldsymbol{\omega}}(-\mathbf{k}',t)$ over spherical shells of width $\Delta k = 1$ ($\boldsymbol{\omega} = \nabla\times\mathbf{u}$ is the vorticity).

The truncated Euler equation dynamics is expected to reach at large times an absolute equilibrium that is a statistically stationary gaussian exact solution of the associated Liouville equation [12]. When the flow has a non vanishing helicity, the absolute equilibria of the kinetic energy and helicity predicted by Kraichnan [13] are

$$E(k) = \frac{k^2}{\alpha}\frac{4\pi}{1-\beta^2k^2/\alpha^2}\;;\;\; H(k) = \frac{k^4\beta}{\alpha^2}\frac{8\pi}{1-\beta^2k^2/\alpha^2}; \tag{3}$$

where $\alpha > 0$ and $\beta k_{\rm max} < \alpha$ to ensure integrability. The values of α and β are uniquely determined by the total amount of energy and helicity (verifying $|H| \le 2k_{\rm max}E$) contained in the wavenumber range $[1, k_{\rm max}]$ [13].

It has been discovered recently that the transient period during which the ideal truncated system reaches equilibrium can mimic forced and dissipative systems. It was originally suggested by Kraichnan and Chen [14] that, considering spatial modes that have not yet thermalized, conservative truncated systems can behave as dissipative ones. The underlying idea is that high wavenumber thermalized modes can act as an energy sink for low wavenumber modes, which will thus behave as if the turbulent flow was viscous. This idea was put on solid ground by calculating the turbulent viscosity caused by thermalized modes and confirmed numerically in high-resolution simulations of the Euler equation in [15]. In these simulations, the energy that was initially concentrated at low wave numbers was found to cascade down to larger wave numbers. A long transient was observed before the system reached full thermalization (details are given in [6]). These results were then extended to helical hydrodynamic flows [11]. Fig. 1 shows the time-evolution of the energy and helicity spectra, compensated by $k^{5/3}$, obtained by the truncated Euler dynamics (2) evolving from a so-called ABC (Arnold, Beltrami and Childress) helical initial data (see Ref. [11] for details). The figure, that is extracted from the data of Ref. [11], clearly display cascade ranges followed by progressive thermalized ranges similar to that obtained in Cichowlas et al. [10] but here with the non zero helicity also cascading to the right.

2.2. An algorithm to generate absolute equilibrium

Absolute-equilibrium solutions have also been examined in compressible flows. In Ref. [6] a stochastic process was constructed with a probability distribution converging to the absolute equilibrium. This construction is necessary in the case of compressible systems because,

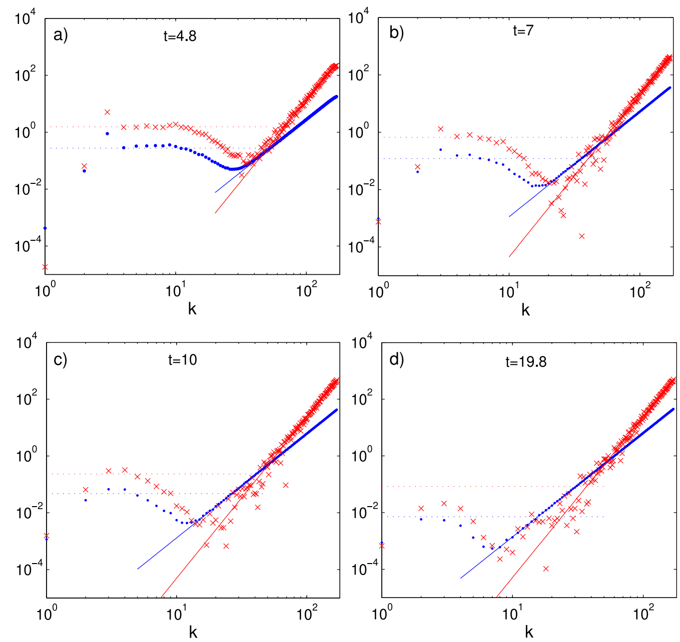

Fig. 1. Compensated energy (•••) and helicity spectra (×××) with thermalized range predictions (3) in solid lines and cascade range predictions in dotted lines. (a) $t = 4.8$. (b) $t = 7$. (c) $t = 10$. (d) $t = 19.8$.

as the conserved energy is at least cubic in the field variables, the associate absolute equilibrium is non-gaussian and cannot be trivially generated as done above (see Eqs. (3)) in the case of incompressible flows.

In the particular case of a canonical system with Hamiltonian given by $H(p_\mu, q^\mu)$ and canonical equations

$$\dot{q}^\mu = \frac{\partial H}{\partial p_\mu}$$
$$\dot{p}_\mu = -\frac{\partial H}{\partial q^\mu}, \tag{4}$$

the stationary probability corresponding to absolute equilibrium is given by the Boltzmann weight

$$P_{st} = Z^{-1}\exp(-\beta H). \tag{5}$$

In this case, the stochastic process with a probability distribution converging to the absolute equilibrium is simply the gradient Langevin dynamics

$$\dot{q}^\mu = -\frac{\partial H}{\partial q^\mu} + \sqrt{\frac{2}{\beta}}\xi_1^\mu$$
$$\dot{p}_\mu = -\frac{\partial H}{\partial p_\mu} + \sqrt{\frac{2}{\beta}}\xi_2^\mu, \tag{6}$$

with the white Gaussian forcing term $\xi_s^\mu(t)$ satisfying

$$\langle \xi_s^\mu(t)\rangle = 0$$
$$\langle \xi_s^\mu(t)\xi_{s'}^\nu(t')\rangle = \delta(t-t')\delta_{ss'}\delta^{\mu\nu}. \tag{7}$$

By considering the associated Fokker–Planck equation [16,17], it is straightforward to show that the stochastic process defined in Eqs (6) and (7) admit the Boltzmann distribution (5) as a stationary probability.

2.3. Thermalization in the Gross–Pitaevskii equation

The study of equilibrium properties and dynamics of the (truncated) Gross–Pitaevskii equation was motivated by our previously obtained results on the $3D$ incompressible Euler equation and was made possible, due to the cubic non-linearity of the Gross–Pitaevskii equation, by the new compressible algorithms of Ref. [6].

We then clarified the previous results concerning the nature of the phase transition that is present in the 3D Gross–Pitaevskii equation by showing that it is a standard second-order transition [18]. Moreover, we showed that the dynamics of thermalization presents a dispersive bottleneck which slows down the thermalization [19]. We have also shown that most of the standard mutual friction phenomenology applies to the interaction of vortices with the normal fluid present in the finite temperature equilibrium. However, we found an exception to this agreement, due to an effect caused by thermally induced Kelvin waves which produce an anomalous translation velocity for vortex rings [20]. This latter result was found to depend solely on the hydrodynamic effect of thermally excited Kelvin waves. These results have been reviewed in Ref. [21]. Later, an in-depth study of the 2D Gross–Pitaevskii equation confirmed the slowing down of thermalization by a dispersive bottleneck. Moreover, full thermalization was achieved and, considering finite size effects, the correlation functions and spectra were found to be consistent with their non-trivial Berezinskii–Kosterlitz–Thouless values [22]. A generalized framework was proposed in Ref. [23]. The standard framework was later applied to study finite-temperature effects in helical quantum turbulence in Ref. [24]. Quantitative estimation of effective viscosity in quantum turbulence were given in Ref. [25]. The method was applied in an astrophysical context to the formation of compact objects at finite temperatures in a dark-matter-candidate self-gravitating bosonic system in Ref. [26] and to quantum walks in Ref. [27].

2.4. Applications of thermalization process to classical systems

Thermalization in magnetohydrodynamic systems were studied in Ref. [29]. and [30]. Dynamo action by turbulence in absolute equilibrium was investigated in Ref. [31].

An effect, very similar to the slowing down of thermalization by a dispersive bottleneck first noticed in Ref. [19], was also observed in a model of (incompressible) classical turbulence in Ref. [32]. Statistical reversals in two-dimensional confined turbulent flows were studied in Ref. [33], with more general results reviewed in Ref. [34]. The thermal equilibrium state of large-scale viscous flows forced at small scale was investigated in Ref. [35,36]. Turbulent cascade, bottleneck, and thermalized spectrum in hyperviscous flows were studied in Ref. [37].

Finally the algorithms of Ref. [6] were applied to point vortex models in Refs. [38,39], in the context of Levy on-off intermittency.

2.5. Thermalization and tygers in the inviscid Burgers equation

The particular case of the inviscid truncated Burgers equation will be examined in detail in Section 3 below in the context of time-correlation functions and their crossover to Kardar–Parisi–Zhang scaling when viscosity and noise are added to the inviscid Burgers equation. However before doing this I think that it is important to mention a recently discovered phenomenon that was dubbed as "tygers" in studies of the two-dimensional Euler and the Burgers equations [40]. The curious fact is that the first "spurious" effects of thermalization in physical space do not occur near the shock, but away from it. Sharp localized structures, the so-called tygers, are formed. After collapsing, thermalization starts to take place near the location of the tyger, eventually expanding to the whole domain (see Fig. 2). The mechanism behind the formation of a tyger has been identified as a resonant interaction between fluid particles and truncation noise [40]. More details are given in Ref. [28].

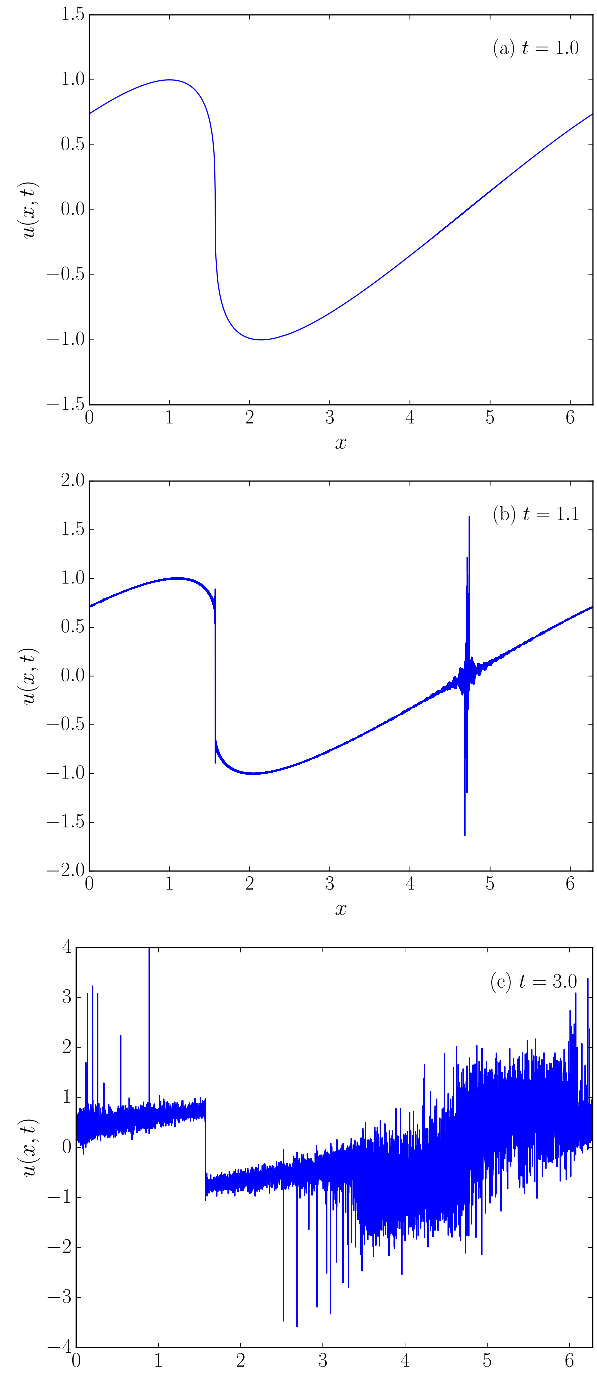

Fig. 2. Evolution of the numerical solution $u(x,t)$ of the inviscid Burgers equation with spectral truncation performed at $k = 5461$. The initial data is $u(x,0) = \cos(x)$ and the solution $u(x,t)$ is shown at different times: (a) $t = 1.0$, (b) $t = 1.1$, (c) $t = 3.0$. The shock is formed at $t = 1$, and the tyger has developed and started to collapse at $t = 1.1$. See Ref. [28] for more details.

3. Crossover to Kardar–Parisi–Zhang scaling

This section is devoted to the collaboration that resulted in the publication of Ref. [7]. I first recall the basic definitions that relate the 1D Burgers equation to the Kardar–Parisi–Zhang (KPZ) system. Then, I discuss spectral truncation, conserved quantities and the corresponding stationary probability. After a brief discussion of the physical parameters the main results on the crossover are given.

3.1. System definitions

Consider the generalized randomly forced $1D$ Burgers equation (with spectral power-law forcing) which is defined by the following stochastic process for the velocity field $u(x,t)$ (see Refs. [41–45]):

$$\partial_t u + \lambda u \partial_x u = \nu \partial_{xx} u + \sqrt{D}\partial_x f, \tag{8}$$

where λ is the coefficient of the nonlinear term, ν is the kinematic viscosity, D a diffusion coefficient and f is a zero-mean Gaussian force with variance

$$\langle f(x,t) f(x',t')\rangle = 2\pi\delta(x-x')\delta(t-t'). \tag{9}$$

Defining the so-called interface height h by

$$h(x,t) = \int_{x_0}^{x} u(y,t)dy, \tag{10}$$

where x_0 plays the role of a (possibly time-dependent: see Ref. [46]) constant of integration (thus $u = \partial_x h$) we obtain the Kardar–Parisi–Zhang (KPZ) equation [42,47–49] for h which reads

$$\partial_t h + \frac{\lambda}{2}(\partial_x h)^2 = \nu \partial_{xx} h + \sqrt{D} f, \tag{11}$$

where we have omitted a spatial constant in the noise term f that is needed for mathematical consistency [50] and can also be used to absorb the time-dependency of the integration constant in (10). In the following, 2 particular cases are considered: (i) The deterministic, inviscid $1D$ Burgers equation, with $\lambda = 1$, $\nu = 0$, and $D = 0$; (ii) the linear Edwards–Wilkinson (EW) equation [51], with $\lambda = 0$, $\nu > 0$ and $D > 0$. The general case is the 1D KPZ Eq. (11), with $\lambda > 0$, $\nu > 0$ and $D > 0$.

3.2. Spectral truncation and conserved quantities

Consider 2π-periodic boundary conditions in x and introduce the Fourier representation

$$u(x,t) = \sum_{k=-\infty}^{\infty} \hat{u}(k,t)\exp(ikx). \tag{12}$$

As $u(x,t)$ is real, its Fourier transform $\hat{u}(k,t)$ satisfies $\hat{u}(-k,t) = \overline{\hat{u}(k,t)}$ (with complex conjugation shown by an overline). Using

$$\frac{u^2(x,t)}{2} = \frac{1}{2}\sum_{n,p=-\infty}^{\infty} \hat{u}_{n-p}(t)\hat{u}_p(t)e^{inx}, \tag{13}$$

the non-forced, non-viscous Burgers equation (Eq. (8) with $\nu = 0$, $\lambda = 1$ and $D = 0$) can be written as

$$\partial_t \hat{u}(k,t) = -\frac{ik}{2}\sum_{p=-\infty}^{\infty} \hat{u}_{k-p}(t)\hat{u}_p(t). \tag{14}$$

Eq. (14) conserves the total energy

$$\begin{aligned} E &= \frac{1}{2\pi}\int_0^{2\pi} \frac{u(x,t)^2}{2}dx \\ &= \frac{1}{2}\sum_{k=-\infty}^{\infty} |\hat{u}(k,t)|^2. \end{aligned} \tag{15}$$

Integration by parts of the nonlinear term in (8) shows that the integrals

$$I_n(t) = \int_0^{2\pi} u(x,t)^n dx, \tag{16}$$

are all conserved by the (untruncated) inviscid dynamics (14), with the energy (15) corresponding to the special case $n = 2$.

Spectrally truncating this system amounts to *imposing* that, for $k > k_{\rm max}$, $\hat{u}(k,t) = 0$ and $\partial_t \hat{u}(k,t) = 0$. Namely, we introduce the Galerkin projector $\mathcal{P}$ which reads in Fourier space

$$\mathcal{P}_{\rm G}[\hat{u}_k] = \theta(k_{\rm max} - |k|)\hat{u}_k, \tag{17}$$

where $\theta(k) = 1$, if $k \le k_{\rm max}$ and $\theta(k) = 0$, if $k > k_{\rm max}$. Thus, truncation amounts to replacements $u := \mathcal{P}_{\rm G}[u]$, $u\partial_x u := \mathcal{P}_{\rm G}[u\partial_x u]$ and $f := \mathcal{P}_{\rm G}[f]$ in Eq. (8), thus reducing (14) to a finite number of ordinary differential equations.

Applying the replacements, the spectrally truncated version of (14) yields

$$\partial_t \hat{u}(k,t) = \mathcal{N}_k(\hat{u}), \tag{18}$$

where the nonlinear truncated term $\mathcal{N}_k(\hat{u})$ is given by:

$$\mathcal{N}_k(\hat{u}) = -\frac{ik}{2}\sum_{p,q}\delta_{k,p+q}\theta(k_{\rm max}-|k|)\theta(k_{\rm max}-|p|)\theta(k_{\rm max}-|q|)\hat{u}_p\hat{u}_q, \tag{19}$$

(δ denotes the Kronecker symbol).

It is easy to check that the nonlinear term (19) satisfies the following relations

$$\begin{aligned} 0 &= \mathcal{N}_0(\hat{u}), \\ 0 &= \sum_k \hat{u}_{-k}\mathcal{N}_k(\hat{u}), \\ 0 &= \sum_{k,p,q}\delta_{-k,p+q}\theta(k_{\rm max}-|p|)\theta(k_{\rm max}-|q|)\hat{u}_p\hat{u}_q\mathcal{N}_k(\hat{u}). \end{aligned} \tag{20}$$

Thus, only three of the conservation laws (16) survive Galerkin truncation and

$$\begin{aligned} P &= \hat{u}_0, \\ E &= \frac{1}{2}\sum_{k=-k_{\rm max}}^{k_{\rm max}} |\hat{u}(k,t)|^2, \text{ and} \\ H &= \sum_{k,p,q}\delta_{-k,p+q}\theta(k_{\rm max}-|k|)\theta(k_{\rm max}-|p|)\theta(k_{\rm max}-|q|) \\ &\quad \hat{u}_k\hat{u}_p\hat{u}_q, \end{aligned} \tag{21}$$

are *still* exactly conserved after truncation.

The conserved quantities P and E are respectively the momentum and the energy of the system. The third surviving conserved quantity H can be used to provide an explicit Hamiltonian formulation of the truncated system and is known to play a role in thermalization dynamics only for very particular choices of initial conditions [52].

Standard Fourier pseudospectral method with dealiasing performed by the 2/3 rule are identical to a spectral Galerkin method (see, for example, Ref. [8]). Using N collocation points, spectral truncation must be performed for $k > k_{\rm max} = \lfloor N/3 \rfloor$, where $\lfloor\cdot\rfloor$ denotes the floor function. Note that with this dealiasing choice, the third conserved quantity H must be evaluated as $\mathcal{P}_{\rm G}[u\mathcal{P}_{\rm G}[u^2]]$.

3.3. Stationary probabilities

The nonlinear truncated term (19) obeys the Liouville property

$$\sum_k \frac{\partial \mathcal{N}_k(\hat{u})}{\partial \hat{u}_k} = 0. \tag{22}$$

It is generally argued (see *e.g.* Refs. [1,4,5]) in the case of absolute equilibrium of the (inviscid deterministic $1D$ truncated) Burgers equation that the microcanonical distribution

$$P_{\rm mc}[u] = Z_{\rm mc}^{-1}\delta(E(u)-E), \tag{23}$$

when the number of degrees of freedom $2k_{\rm max}+1$ is large enough, can be well approximated by the canonical distribution

$$P_{\rm sta}[u] = Z_{\rm c}^{-1}e^{-\beta E}, \tag{24}$$

where $Z_{\rm mc}$ and $Z_{\rm c}$ denote normalization factors. A more direct way to proceed is to introduce the Liouville equation for the probability $\mathbb{P}\left[\{\hat{u}_k,\hat{u}_k^*\}_{0<k\le k_{\rm max}}\right]$,

$$\frac{\partial \mathbb{P}}{\partial t} = \sum_{0<k\le k_{\rm max}} \frac{\partial}{\partial \hat{u}_k}\left[-\mathcal{N}_k(\hat{u})\mathbb{P}\right] + c.c\,, \tag{25}$$

where $\hat{u}^*_k = \hat{u}_{-k}$ is considered as an independent variable and $c.c$ denotes a complex conjugation. Note that there is only one independent variable at $k = 0$ with trivial dynamics as the corresponding nonlinear term vanishes (see the first of Eqs. (20)).

It follows directly from the conservation of energy that (25) admits (24) as a stationary solution.

Note that the stationary distribution (24) is a white noise in space for $u(x)$ and therefore a Brownian process for $h(x)$.

In both cases EW ($\lambda = 0$, $\nu > 0$ and $D > 0$) and KPZ ($\lambda > 0$, $\nu > 0$ and $D > 0$) the probability distribution $\mathbb{P}$ of the stochastic process defined by the equations. (8)–(9) and spectral truncation (17) can be shown to obey the following Fokker–Planck equation [16,17]

$$\frac{\partial \mathbb{P}}{\partial t} = \sum_{0<k\leq k_{\max}} \frac{\partial}{\partial \hat{u}_k}\left[-(\lambda \mathcal{N}_k(\hat{u}) - \nu k^2 \hat{u}_k)\mathbb{P} + Dk^2 \frac{\partial \mathbb{P}}{\partial \hat{u}^*_k}\right] + c.c\,. \tag{26}$$

Note that (24) is also a stationary solution of (26). Indeed, the nonlinear term of the Fokker–Planck equation can be treated exactly like its counterpart in the Liouville Eq. (25); the remaining terms also vanish for the stationary distribution (24), because, at equilibrium, we must have $\nu k^2 \hat{u}_k - \beta D k^2 \hat{u}_k = 0$, from which we obtain

$$D = \frac{\nu}{\beta}. \tag{27}$$

Defining the *r.m.s.* velocity $u_{\rm rms}$ by averaging over the stationary distribution (24)

$$\langle E \rangle = \frac{u^2_{\rm rms}}{2} = \frac{k_{\max}+1}{\beta}, \tag{28}$$

(see Eqs. (15) and (17)) we find that

$$\beta = \frac{2(k_{\max}+1)}{u^2_{\rm rms}}, \tag{29}$$

$$D = \frac{\nu u^2_{\rm rms}}{2(k_{\max}+1)}. \tag{30}$$

These last relations determined the equilibrium probability. Thus, the non-trivial aspect of the dynamics concerns the temporal correlation functions

$$\Gamma(k,\tau) = \langle \hat{u}^*_k(t)\hat{u}_k(t+\tau)\rangle_t. \tag{31}$$

In the KPZ case, with the Fokker–Planck Eq. (26), it is well known [41, 42] that the existence of a fluctuation dissipation theorem ensures that the associated response function has the same time-scale characteristic as the equilibrium time correlation function. The same fluctuation–dissipation relation (with statistical averaging on the initial conditions) [53] also applies in the inviscid and noiseless case (25).

3.4. Algorithms and physical parameters

Details on algorithms: the pseudospectral method, time stepping and averaging method are given in Ref. [7].

As 2π-periodic boundary conditions are used, the largest scale L in our simulations is always fixed at $L = 2\pi$. The smallest available scales are resolution-dependent and are related to the largest wave number $k_{\max} = \lfloor N/3 \rfloor$ (which is equivalent to the inverse of the size of the spatial mesh $\Delta x = 2\pi/N$, where N indicates the resolution). Thus, a given calculation is parameterized by $u_{\rm rms}$, $k_{\max}$ and ν.

The initial data used to start time integrations is always set to be a random gaussian field (see (24) and (28)) and the same $u_{\rm rms}$ is used to set D to its viscosity and resolution dependent value (30). Thus, the case $\nu = 0$ (and $D = 0$) amounts to integrating the inviscid truncated Burgers equation from an initial conditions of absolute equilibrium corresponding to $u_{\rm rms}$. When ν is non-zero, the full KPZ system (9) (with $\lambda = 1$) is integrated, also starting from the same equilibrium distribution.

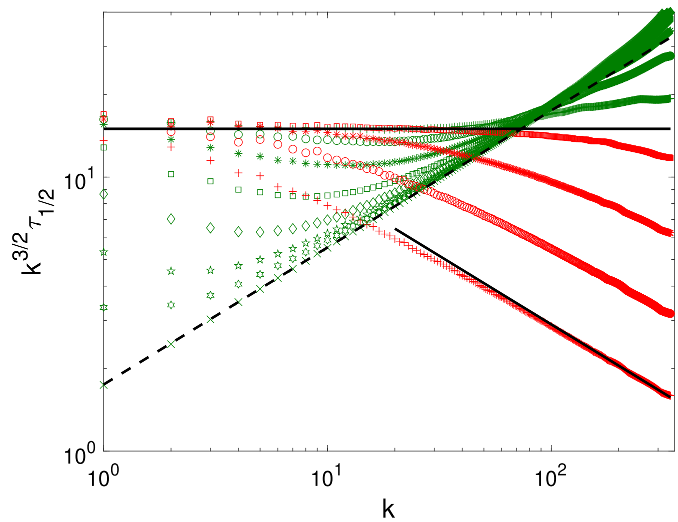

Fig. 3. Crossover in the scaling of the decorrelation time $\tau_{\frac{1}{2}}$ compensated by $k^{3/2}$: $k^{3/2}\tau_{\frac{1}{2}}$ versus k. Red markers correspond to the EW to KPZ transition: $\nu = 2.4 \times 10^{-2}$: +, $\nu = 1.2 \times 10^{-2}$: o, $\nu = 6.0 \times 10^{-3}$: asterisk and $\nu = 3.0 \times 10^{-3}$: square. Green markers correspond to the KPZ to inviscid transition: $\nu = 1.5 \times 10^{-3}$: +, $\nu = 7.5 \times 10^{-4}$: o, $\nu = 3.8 \times 10^{-4}$: asterisk, $\nu = 1.9 \times 10^{-4}$: square, $\nu = 9.4 \times 10^{-5}$: diamond, $\nu = 4.7 \times 10^{-5}$: pentagram, $\nu = 2.3 \times 10^{-5}$: hexagram, and $\nu = 0$: cross. Scaling laws are indicated by solid lines: EW k^{-2} and KPZ $k^{-3/2}$. The new inviscid k^{-1} scaling is denoted by a dashed line. Runs performed with $k_{\max} = 341$ and $u_{\rm rms} = 1$. (For interpretation of the references to colour in this figure legend, the reader is referred to the web version of this article.)

3.5. Scalings and numerical determination of crossover behaviour

We now introduce a scale-dependent Reynolds number: in the inviscid limit, the typical relaxation time near the absolute equilibrium can be studied conveniently via the scale-dependent correlation time $\tau_{1/2}(k)$, which can be computed from the time-dependent correlation function (31) by solving $\Gamma(k,\tau_{1/2}) = \Gamma(k,0)/2$. It is known to scale as $\tau_{1/2}(k) \sim k^{-1}$ [54–56]. Note that the same k^{-1} scaling law is known to take place in the truncated $3D$ Euler equation [10]. Thus $\tau_{1/2}(k)$ cannot be simply related to an eddy turnover time defined from the equilibrium energy spectrum that scales as $E(k) \sim k^{d-1}$ in d-dimensions.

As demonstrated above (see (26)), the $1D$ KPZ equation admits the same exact equilibrium probability distribution as the inviscid Burgers equation However, the $1D$ KPZ correlation time around equilibrium is known to have a $k^{-3/2}$ scaling. Thus two different time-correlation scalings k^{-1} and $k^{-3/2}$ around the same equilibrium are expected for the inviscid truncated Burgers equation and the KPZ equation. Also there is a third (trivially linear) viscous scaling: the EW k^{-2} scaling that arises when the effect of the nonlinear term is negligible.

In a general case, because of renormalization group arguments [41, 42], we expect to find the KPZ scaling of the correlation time in the limit of the large spatial scales. However, the speed of this approach is expected to depend on the value of small-scale parameters. Defining the Reynolds number at wave number k by $R_e(k) = u_{\rm rms}/(\nu k)$, The Reynolds number at truncation scale is given by $R_{\min} = R_e(k_{\max})$: $R_{\min} = u_{\rm rms}/(\nu k_{\max})$ or

$$R_{\min} = \frac{3}{N\nu} u_{\rm rms}. \tag{32}$$

Thus, we expect to see EW scaling when $R_{\min} \ll 1$ and recover the inviscid truncated Burgers case in the limit $R_{\min} \to \infty$ that corresponds to $\nu = 0$. Fixing the time-scale by setting $u_{\rm rms} = 1$, we now study the crossover in terms of the dimensionless parameter $R_{\min}$ by varying ν.

The crossover behaviour is clearly visible in Fig. 3 which shows the correlation time compensated by $k^{3/2}$, so that the KPZ scaling corresponds to a horizontal line. The red markers correspond to the

EW to KPZ transition with different values of viscosities in geometric progression corresponding to Reynolds numbers at truncation scale: $R_{\min} = 0.12$, $R_{\min} = 0.24$, $R_{\min} = 0.48$ and $R_{\min} = 0.96$. The green markers correspond to the KPZ to inviscid transition, with different viscosities, also in geometric progression corresponding to Reynolds numbers: $R_{\min} = 1.96$, $R_{\min} = 3.91$, $R_{\min} = 7.71$, $R_{\min} = 15.4$, $R_{\min} = 31.2$, $R_{\min} = 62.3$, $R_{\min} = 124.6$ and $R_{\min} = \infty$. The EW k^{-2} scaling law and the KPZ $k^{-3/2}$ scaling are indicated by solid lines and the inviscid k^{-1} scaling scale is indicated by a dotted line.

4. Conclusion

After reviewing the collaborations that went on during a decade and finally led to the joint work that was published in Ref. [7], I gave a short description of the main result of this work.

We found a new crossover, governed by the truncated scale Reynolds number $R_{\min}$, towards the inviscid state where the correlation time scales as k^{-1}. This new scaling corresponds to the absolute equilibrium solution of the inviscid and noiseless Burgers equation. To address this new scaling by a renormalization group analysis would require to find, in addition to the known [42] KPZ stable fixed points and EW unstable fixed points, a new unstable fixed point corresponding to an inviscid $R_{\min} = \infty$ (or $\lambda = \infty$) value of the parameters. This point is left for further work.

Declaration of competing interest

The authors declare that they have no known competing financial interests or personal relationships that could have appeared to influence the work reported in this paper.

Data availability

Data will be made available on request.

Acknowledgements

The work mentioned in this article was performed in collaboration with R. Agrawal, A. Alexakis, N. G. Berloff, C. Cartes, C. Cichowlas, P. Clark Di Leoni, F. Debbasch, S. Fauve, G. Di Molfetta, G. Krstulovic, P. D. Mininni, R. Pandit, A. Pouquet, S. G. G. Prasath, N. P. Proukakis, S. S. Ray, V. Shukla, E. Tirapegui, L. Tuckerman, A. van Kan and A. K. Verma.

This work was supported by the French Agence nationale de la recherche (ANR QUTE-HPC project No. ANR-18-CE46-0013). This work was granted access to HPC resources of MesoPSL financed by Region Ile de France and the project Equip@Meso (reference ANR-10-EQPX-29-01) of the programme Invsessements d'Avenir supervised by Agence Nationale pour la Recherche. I thank the Indo-French Centre for Applied Mathematics for financial support.

References

[1] Lee TD. On some statistical properties of hydrodynamical and magneto-hydrodynamical fields. Quart Appl Math 1952;10(1):69–74.
[2] Hopf E. Statistical hydromechanics and functional calculus. J Ration Mech Anal 1952;1:87–123.
[3] Kraichnan R. On the statistical mechanics of an adiabatically compressible fluid. J Acoust Soc Am 1955;27(3):438–41.
[4] Kraichnan R. Helical turbulence and absolute equilibrium. J Fluid Mech 1973;59:745–52.
[5] Orszag S. Statistical theory of turbulence. In: Balian R, Peube JL, editors. Les Houches 1973: fluid dynamics. New York: Gordon and Breach; 1977.
[6] Krstulovic G, Cartes C, Brachet M, Tirapegui E. Generation and charaterization of absolute equilibrium of compressible flows. Int J Bifurcation Chaos 2009;19(10):3445–59. http://dx.doi.org/10.1142/S021812740902489X.
[7] Cartes C, Tirapegui E, Pandit R, Brachet M. The Galerkin-truncated Burgers equation: Crossover from inviscid-thermalized to Kardar-Parisi-Zhang scaling. Phil Trans R Soc A 2022;380(2219):20210090. http://dx.doi.org/10.1098/rsta.2021.0090.
[8] Gottlieb D, Orszag SA. Numerical analysis of spectral methods. Philadelphia: SIAM; 1977.
[9] Canuto C, Hussani MY, Quarteroni A, Zang TA. Spectral methods in fluid dynamics. New York and Berlin: Springer-Verlag; 1988.
[10] Cichowlas C, Bonaïti P, Debbasch F, Brachet M. Effective dissipation and turbulence in spectrally truncated Euler flows. Phys Rev Lett 2005;95(26):264502.
[11] Krstulovic G, Mininni PD, Brachet ME, Pouquet A. Cascades, thermalization, and eddy viscosity in helical Galerkin truncated Euler flows. Phys Rev E 2009;1–5.
[12] Orszag S. Analytical theories of turbulence. J Fluid Mech 1970;41(363).
[13] Kraichnan R. Helical turbulence and absolute equilibrium. J Fluid Mech 1973;59:745–52.
[14] Kraichnan RH, Chen S. Is there a statistical mechanics of turbulence? Physica D 1989;37(1):160–72.
[15] Cichowlas C, Bonaïti P, Debbasch F, Brachet M. Effective dissipation and turbulence in spectrally truncated Euler flows. Phys Rev Lett 2005;95(26).
[16] Langouche F, Roekaerts D, Tirapegui E. Functional integration and semiclassical expansions. D Reidel Publishing Compagny; 1982.
[17] van Kampen NG. Stochastic processes in physics and chemistry. North-Holland: Elsevier; 1981.
[18] Krstulovic G, Brachet M. Energy cascade with small-scale thermalization, counterflow metastability, and anomalous velocity of vortex rings in Fourier-truncated Gross-Pitaevskii equation. Phys Rev E 2011;83:066311. http://dx.doi.org/10.1103/PhysRevE.83.066311.
[19] Krstulovic G, Brachet M. Dispersive bottleneck delaying thermalization of turbulent Bose-Einstein condensates. Phys Rev Lett 2011;106:115303. http://dx.doi.org/10.1103/PhysRevLett.106.115303.
[20] Krstulovic G, Brachet M. Anomalous vortex-ring velocities induced by thermally excited Kelvin waves and counterflow effects in superfluids. Phys Rev B 2011;83:132506. http://dx.doi.org/10.1103/PhysRevB.83.132506.
[21] Brachet M. Gross-Pitaevskii description of superfluid dynamics at finite temperature: A short review of recent results. C R Phys 2012;13(9):954–65. http://dx.doi.org/10.1016/j.crhy.2012.10.006.
[22] Shukla V, Brachet M, Pandit R. Turbulence in the two-dimensional Fourier-truncated Gross-Pitaevskii equation. New J Phys 2013;15(11):113025. http://dx.doi.org/10.1088/1367-2630/15/11/113025.
[23] Berloff NG, Brachet M, Proukakis NP. Modeling quantum fluid dynamics at nonzero temperatures. Proc Natl Acad Sci 2014;111(1):4675–82. http://dx.doi.org/10.1073/pnas.1312549111.
[24] Clark Di Leoni P, Mininni PD, Brachet ME. Finite-temperature effects in helical quantum turbulence. Phys Rev A 2018;97:043629. http://dx.doi.org/10.1103/PhysRevA.97.043629.
[25] Shukla V, Mininni PD, Krstulovic G, di Leoni PC, Brachet ME. Quantitative estimation of effective viscosity in quantum turbulence. Phys Rev A 2019;99:043605. http://dx.doi.org/10.1103/PhysRevA.99.043605.
[26] Verma AK, Pandit R, Brachet ME. Formation of compact objects at finite temperatures in a dark-matter-candidate self-gravitating bosonic system. Phys Rev Res 2021;3:L022016. http://dx.doi.org/10.1103/PhysRevResearch.3.L022016.
[27] Di Molfetta G, Debbasch F, Brachet M. Nonlinear optical Galton board: Thermalization and continuous limit. Phys Rev E 2015;92:042923. http://dx.doi.org/10.1103/PhysRevE.92.042923.
[28] Clark Di Leoni P, Mininni PD, Brachet ME. Dynamics of partially thermalized solutions of the Burgers equation. Phys Rev Fluids 2018;3:014603. http://dx.doi.org/10.1103/PhysRevFluids.3.014603.
[29] Krstulovic G, Brachet M-E, Pouquet A. Alfvén waves and ideal two-dimensional Galerkin truncated magnetohydrodynamics. Phys Rev E 2011;84:016410. http://dx.doi.org/10.1103/PhysRevE.84.016410.
[30] Stawarz JE, Pouquet A, Brachet M-E. Long-time properties of magnetohydrodynamic turbulence and the role of symmetries. Phys Rev E 2012;86:036307. http://dx.doi.org/10.1103/PhysRevE.86.036307.
[31] Prasath SGG, Fauve S, Brachet M. Dynamo action by turbulence in absolute equilibrium. EPL (Europhys Lett) 2014;106(2):29002. http://dx.doi.org/10.1209/0295-5075/106/29002.
[32] Di Molfetta G, Krstulovic G, Brachet M. Self-truncation and scaling in Euler-Voigt-α and related fluid models. Phys Rev E 2015;92:013020. http://dx.doi.org/10.1103/PhysRevE.92.013020.
[33] Shukla V, Fauve S, Brachet M. Statistical theory of reversals in two-dimensional confined turbulent flows. Phys Rev E 2016;94:061101. http://dx.doi.org/10.1103/PhysRevE.94.061101.
[34] Pandit R, Banerjee D, Bhatnagar A, Brachet M, Gupta A, Mitra D, et al. An overview of the statistical properties of two-dimensional turbulence in fluids with particles, conducting fluids, fluids with polymer additives, binary-fluid mixtures, and superfluids. Phys Fluids 2017;29(11):111112. http://dx.doi.org/10.1063/1.4986802.
[35] Alexakis A, Brachet M-E. On the thermal equilibrium state of large-scale flows. J Fluid Mech 2019;872:594–625. http://dx.doi.org/10.1017/jfm.2019.394.
[36] Alexakis A, Brachet M-E. Energy fluxes in quasi-equilibrium flows. J Fluid Mech 2020;884:A33. http://dx.doi.org/10.1017/jfm.2019.965.

[37] Agrawal R, Alexakis A, Brachet ME, Tuckerman LS. Turbulent cascade, bottleneck, and thermalized spectrum in hyperviscous flows. Phys Rev Fluids 2020;5:024601. http://dx.doi.org/10.1103/PhysRevFluids.5.024601.

[38] van Kan A, Alexakis A, Brachet M-E. Intermittency of three-dimensional perturbations in a point-vortex model. Phys Rev E 2021;103:053102. http://dx.doi.org/10.1103/PhysRevE.103.053102.

[39] van Kan A, Alexakis A, Brachet M-E. Lévy on-off intermittency. Phys Rev E 2021;103:052115. http://dx.doi.org/10.1103/PhysRevE.103.052115.

[40] Ray SS, Frisch U, Nazarenko S, Matsumoto T. Resonance phenomenon for the Galerkin-truncated Burgers and Euler equations. Phys Rev E 2011;84:016301. http://dx.doi.org/10.1103/PhysRevE.84.016301.

[41] Forster D, Nelson DR, Stephen MJ. Large-distance and long-time properties of a randomly stirred fluid. Phys Rev A 1977;16:732–49. http://dx.doi.org/10.1103/PhysRevA.16.732.

[42] Kardar M, Parisi G, Zhang Y-C. Dynamic scaling of growing interfaces. Phys Rev Lett 1986;56:889–92. http://dx.doi.org/10.1103/PhysRevLett.56.889.

[43] Frisch U. Turbulence: The legacy of a N. Kolmogorov. Cambridge University Press; 1995.

[44] Frisch U, Bec J. Burgulence. In: Lesieur M, Yaglom A, David F, editors. New trends in turbulence. Berlin, Heidelberg: Springer Berlin Heidelberg; 2001, p. 341–83.

[45] Bec J, Khanin K. Burgers turbulence. Phys Rep 2007;447(1):1–66. http://dx.doi.org/10.1016/j.physrep.2007.04.002.

[46] Rodríguez-Fernández E, Cuerno R. Non-KPZ fluctuations in the derivative of the Kardar-Parisi-Zhang equation or noisy Burgers equation. Phys Rev E 2020;101:052126. http://dx.doi.org/10.1103/PhysRevE.101.052126, URL https://link.aps.org/doi/10.1103/PhysRevE.101.052126.

[47] Halpin-Healy T, Zhang Y-C. Kinetic roughening phenomena, stochastic growth, directed polymers and all that aspects of multidisciplinary statistical mechanics. Phys Rep 1995;254(4):215–414.

[48] Halpin-Healy T, Lin Y. Universal aspects of curved, flat, and stationary-state Kardar-Parisi-Zhang statistics. Phys Rev E 2014;89:010103. http://dx.doi.org/10.1103/PhysRevE.89.010103.

[49] Halpin-Healy T, Takeuchi KA. A KPZ cocktail-shaken, not stirred. J Stat Phys 2015;160(4):794–814. http://dx.doi.org/10.1007/s10955-015-1282-1.

[50] Hairer M. Solving the KPZ equation. Ann of Math 2013;559–664.

[51] Edwards SF, Wilkinson DR. The surface statistics of a granular aggregate. Proc R Soc Lond Ser A Math Phys Eng Sci 1982;381(1780):17–31. http://dx.doi.org/10.1098/rspa.1982.0056.

[52] Abramov RV, Kovačič G, Majda AJ. Hamiltonian structure and statistically relevant conserved quantities for the truncated Burgers-Hopf equation. Comm Pure Appl Math 2003;56(1):1–46. http://dx.doi.org/10.1002/cpa.3032.

[53] Kraichnan R. Classical fluctuation-relaxation theorem. Phys Rev 1959;113(5):1181, 1182.

[54] Majda AJ, Timofeyev I. Remarkable statistical behavior for truncated Burgers-Hopf dynamics. Proc Natl Acad Sci 2000;97(23):12413–7. http://dx.doi.org/10.1073/pnas.230433997, URL https://www.pnas.org/content/97/23/12413.

[55] Majda A, Timofeyev I. Statistical mechanics for truncations of the Burgers-Hopf equation: A model for intrinsic stochastic behavior with scaling. Milan J Math 2002;70(1):39–96. http://dx.doi.org/10.1007/s00032-002-0003-9.

[56] Cichowlas C. Truncated Euler equation: from complex singularities dynamics to turbulent relaxation. (Ph.D. thesis), Universite Pierre et Marie Curie - Paris VI; 2005, https://tel.archives-ouvertes.fr/tel-00070819/document.